

Thermal-induced phase transitions in self-assembled mesostructured films studied by small-angle X-ray scattering

Plinio Innocenzi,^{a*} Luca Malfatti,^a Tongjit Kidchob,^a Paolo Falcaro,^b Stefano Costacurta,^b Massimo Guglielmi,^b Giovanni Mattei,^c Valentina Bello^c and Heinz Amenitsch^d

^aLaboratorio di Scienza dei Materiali e Nanotecnologie, Nanoworld Institute, Dipartimento di Architettura e Pianificazione, Università di Sassari, Palazzo Pou Salid, Piazza Duomo 6, 07041 Alghero (Sassari), Italy, ^bDipartimento di Ingegneria Meccanica, Settore Materiali, Università di Padova, via Marzolo 9, 35131 Padova, Italy, ^cDipartimento di Fisica 'Galileo Galilei', Università di Padova, via Marzolo 8, 35131 Padova, Italy, and ^dInstitute of Biophysics and X-ray Structure Research, Austrian Academy of Sciences, Schmiedelstraße 6, A-8042, Graz, Austria.
E-mail: plinio@uniss.it

Two examples of phase transition in self-assembled mesostructured hybrid thin films are reported. The materials have been synthesized using tetraethoxysilane as the silica source hydrolyzed with or without the addition of methyltriethoxysilane. The combined use of transmission electron microscopy, small-angle X-ray scattering and computer simulation has been introduced to achieve a clear identification of the organized phases. A structural study of the self-assembled mesophases as a function of thermal treatment has allowed the overall phase transition to be followed. The initial symmetries of mesophases in as-deposited films have been linked to those observed in samples after thermal treatment. The monodimensional shrinkage of silica films during calcination has induced a phase transition from face-centered orthorhombic to body-centered cubic. In hybrid films, instead, the phase transition has not involved a change in the unit cell but a contraction of the cell parameter normal to the substrate.

Keywords: SAXS; self-assembly; mesoporous films; phase transition.

1. Introduction

Synchrotron small-angle X-ray scattering (SAXS) has been widely used, in transmission and in grazing-incidence configurations, to study self-assembled mesostructured films deposited *via* dip-coating (Grosso *et al.*, 2002; Soler-Illia *et al.*, 2002; Cagnol *et al.*, 2003). The technique has revealed to be particularly effective for studying *in situ* the self-assembly mechanisms through which, driven by the fast evaporation of the solvent (evaporation-induced self-assembly, EISA) (Lu *et al.*, 1997), the organic micelles assemble to give different organized mesophases (Klotz *et al.*, 2000; Grosso *et al.*, 2003; Doshi *et al.*, 2003).

The formation of the final mesostructure can be divided into two different stages. The first takes place during dip-coating: the micelles organize, and the solvent evaporation induces a phase transition connected with the reorganization of the micelles (Cagnol *et al.*, 2003). In this phase the withdrawal speed and the relative humidity in the deposition chamber dramatically influence the spatial disposition of the micelles. The second stage is observed after the deposition, when drying

or thermal calcination generally induces a phase transformation (Klotz *et al.*, 2000). This transition, which is due to the uniaxial shrinkage of the film, results in a loss of symmetry and the distortion of the unit cell (Besson *et al.*, 2003; Soler-Illia *et al.*, 2002; Kundu *et al.*, 1998; Falcaro *et al.*, 2004). The extent and type of this phase transition is very much dependent on the synthesis parameters, but the templating agent also plays a very important role. Micelles formed by ionic surfactants, such as cetyltrimethylammonium bromide (CTAB), have properties that can be closely compared with 'hard closed spheres'. Tri-block copolymer surfactants form instead micelles with the long polyethylene oxide chains on the surface of a dense core formed by the hydrophobic polypropylene blocks. The micelles formed by three-block copolymers are, therefore, softer and are more easily deformed (McConnell & Gast, 1996). Another important difference is given by the lower temperature necessary to remove the block copolymers with respect to ionic surfactants. This is reflected in a lower degree of condensation of the pore walls and a higher tendency to deformation. Whilst this effect is well documented in self-assembled films, a clear identification of the phase involved is

not easy to achieve. In general, the indexing and identification of the phases is obtained by the distances and the angles of the observed diffraction spots from SAXS. This can be, however, quite often a source of error if the data are not properly processed.

In the present work we show that SAXS, TEM and computer simulation can be used to define a reliable way of identifying the porous mesostructure in amorphous inorganic and hybrid films (Falcaro *et al.*, 2005). An example of mesostructured films with orthorhombic and tetragonal final symmetry will be shown.

2. Samples preparation

A stock solution was prepared by adding (in the following order) ethanol (EtOH), TEOS, water and HCl in the molar ratios TEOS:EtOH:H₂O:HCl = 1:2.78:1.04:56.2 × 10⁻³. The sol was left to react under stirring for 1 h at room temperature. A second solution was prepared by dissolving 1.3 g Pluronic F-127 in 15 cm³ EtOH and 1.5 cm³ acid aqueous solution. Pluronic F-127 block copolymers (EO₁₀₆-PO₇₀-EO₁₀₆) were obtained from Aldrich and used as received. The final sol was obtained by adding 7.7 cm³ of the stock sol to the solution containing the block copolymer. The final solution, with molar ratios TEOS:EtOH:H₂O:HCl:Pluronic F127 = 1:16.3:5.4:56.5 × 10⁻³:5 × 10⁻³, was reacted under stirring for 24 h and then was aged at 301 K for one week. The same procedure was followed using TEOS and MTES in the stock solution. The final molar ratios of the optimized MTES-TEOS mixture were set at TEOS:MTES:EtOH:H₂O:HCl:F127 = 1:0.56:24.48:14.70:0.11:7.6 × 10⁻³.

The silicon wafers, previously cleaned with hydrofluoric acid, water, EtOH and acetone, were dip-coated using the two different solutions. The dip-coating system was a home-built model, specifically designed to be employed for *in situ* measurements to guarantee high withdrawal stability. The substrate was mounted on a fixed rod, while the beaker containing the solution was moved up and down by a moveable stage connected to an electrical engine. In this way the sample remained fixed and the solution was raised and lowered during the dip-coating procedure. The relative humidity in the deposition chamber was set at 40%; the withdrawal speed was set at 15 cm min⁻¹. After the deposition the films were maintained in the deposition chamber for 10 min and then heated at 423 K for 1 h in air. The firing process was carried out in sequence; that is, all of the samples were fired at 333 K, 473 K, 673 K up to the last thermal step at 873 K. The mesostructure, in films deposited on silicon substrates, was investigated using the high-flux grazing-incidence small-angle X-ray scattering (GI-SAXS) apparatus at the Austrian high-flux beamline of the electron storage ring ELETTRA (Trieste, Italy) (Amenitsch *et al.*, 1998), taking for each image the average of ten single acquisitions with 3 s of exposition time. The instrumental grazing angle was set maintaining an incident X-ray beam (wavelength 1.54 Å) smaller than 3°. From the recording of the CCD detector (1024 × 1024 pixels, Photonic Science) the *out of plane*

diffraction maxima were observed. The distance between sample and detector was calibrated with the diffraction pattern of a salt having a known lattice constant [silver behenate, H(CH₂)₂₁COOAg]: it was possible to obtain this distance (991 mm) with a good precision (±1 mm). The beam centre position was set from the least-squares fit of a circle of 40 entered coordinates, corresponding to 40 positions in the silver behenate powder diffraction ring.

Successively, a radial integration of the image intensity was performed, starting from the beam centre (000). Typically, the whole image was masked leaving out the peak of interest and integration was successively made. This procedure allowed us to minimize the peak position errors caused by the overlap of information in diffraction patterns. Knowing the distance between sample and detector, it was possible to calculate 2θ and *d*_{hkl} for each spot and the lattice constants. Supposing that the radially integrated spot intensities fit a Gaussian curve, the uncertainty on the *d*-spacing, calculated from the intensity maximum, was estimated to be ±6% by the FWHM of the curve. FIT2D was used (A. P. Hammersley, ESRF) to analyze the SAXS images.

3. Identification of the mesophases in self-assembled films

Transmission and grazing-incidence SAXS represents a powerful tool for identifying the porous organized phase in self-assembled mesoporous films. This technique has been widely applied both *in situ* during film formation and to study the material evolution during thermal processing. The deposition by evaporation-induced self-assembly of a mesostructured film is followed by a drying process, generally performed at low temperature (~333 K) to evaporate the solvent, and a thermal treatment to stabilize the structure. This treatment can be used at the same time to remove the organic template from the structure by thermal calcination. After drying, the pores are in fact still filled with the surfactant whose removal can cause a partial collapse of the mesostructure if the pore walls are not thick enough or if their degree of condensation is still low. In Fig. 1 the FTIR

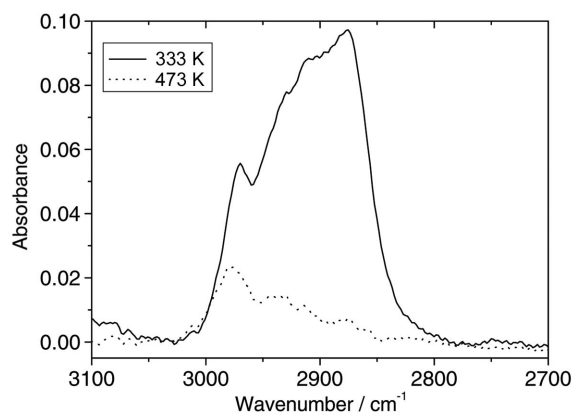


Figure 1
FTIR absorption spectra of MTES-TEOS films after drying at 333 K and after thermal calcination at 473 K.

absorption spectra of self-assembled films after drying (333 K) and calcination at 473 K in air are shown. This temperature is high enough to remove most of the surfactant, because block copolymers are easily degraded even at relatively low temperatures. In the wavenumber range of Fig. 1, the typical fingerprint of C–H vibrations in Pluronic is observed (Su *et al.*, 2002). The reduction in absorption area at 473 K indicates that around 85% of the organic template has been removed.

At this temperature, however, the pore walls are not rigid enough to sustain the porous structure. Therefore mono-dimensional shrinkage follows calcination, because the changes in the directions parallel to the substrates are hindered by the adhesion of the film (Yu *et al.*, 2003). This effect not only causes a pure shrinkage of the films, with a reduction in thickness and distortion of pores shape; the transformation induced by the thermal treatment causes, in fact, a distortion of the network structure that allows the identification of a new porous phase. Whilst the formation of the mesophase during EISA is ruled by a complex interaction of several parameters, and epitaxial relationships have been supposed to explain the formation of two-dimensional hexagonal phases from cubic phases (Grosso *et al.*, 2003; Yao *et al.*, 2000), the transitions from dried to calcined films are restricted to those allowed by group theory (Falcaro *et al.*, 2004).

The identification of the mesophase is, however, quite difficult to achieve even in the dried and calcined films, where

a stationary condition is reached. The difficulty is essentially arisen by the limited number of diffraction spots, splitting of spots owing to grazing-incidence geometry that induces instrumental effects and a lower organization of the film. Fig. 2 shows the SAXS images obtained from films dried at 333 K and calcined at 873 K. Two different sets of samples are shown, the first one obtained from pure TEOS sols which give inorganic (SiO_2) films after thermal treatment (Figs. 2*a* and 2*b*), and the second one from MTES–TEOS sols which give hybrid organic inorganic films (Figs. 2*c* and 2*d*). All the images are in grazing incidence with the exception of Fig. 2(*a*) which is taken in transmission mode. This is, in fact, the only instrumental configuration that allows the identification of a cubic phase. The silica sample (Figs. 2*a* and 2*b*) shows a lower degree of organization, with porous domains within the structure, as also observed by TEM.

Fig. 3 shows the TEM bright-field image of a cross section of a silica film (TEOS samples). The film was calcined at 773 K and the pores, owing to the uniaxial shrinkage, exhibit an elliptical shape. The thickness of the film was 385 ± 5 nm and the measured pore dimensions were 9.3 nm (main axis) and 4.2 nm. The image shows that the periodicity of matter is given by organized porous domains as opposed to crystalline materials where the periodicity is given by the ordered disposition of atoms in a lattice.

The SAXS images were used to identify the mesophases in the dried films (333 K) and after calcination (873 K). The phase transitions observed in the TEOS and MTES–TEOS films are shown in Fig. 4. The TEOS samples show a thermal-induced phase transformation from cubic, $Im\bar{3}m$ (in the space group), to orthorhombic, $Fmmm$, whilst the hybrid MTES–TEOS films exhibit a transition from body-centered tetragonal, $I4/mmm$ (with the cell parameter c orthogonal to the substrate, so that $a < c$), to tetragonal, $I4/mmm$, with $a > c$. It is interesting to observe that the substitution of a part of the silica precursor (tetraethoxysilane) with methyltriethoxysilane

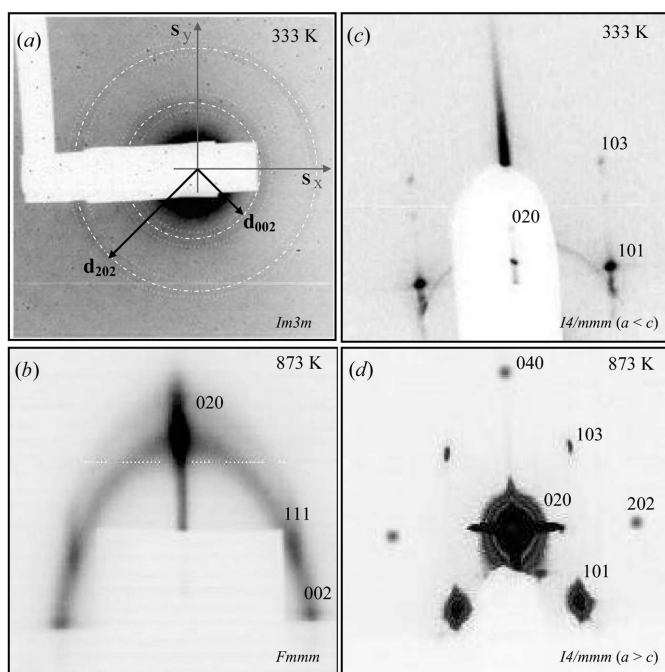


Figure 2

SAXS images of self-assembled films obtained from TEOS (*a*) and (*b*) or MTES–TEOS sols (*c*) and (*d*). The figure shows GISAXS images of films calcined at 873 K (*b*) and (*d*), or after drying at 333 K (*a*) and (*c*). The image (*a*) is shown in transmission to allow identification of the cubic phase. In the image (*d*) the diffraction spots corresponding to the 040, 202 and equivalent label have been added from a measure obtained increasing the exposition time.

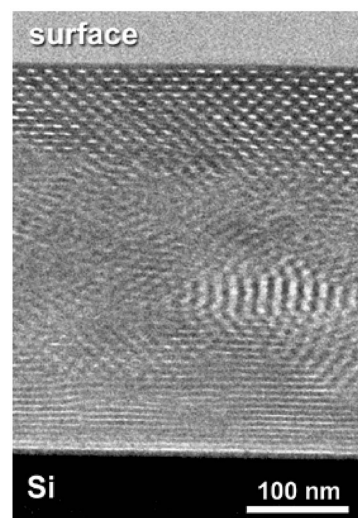


Figure 3

TEM bright-field image of a cross section of a silica film after calcination at 773 K (TEOS samples).

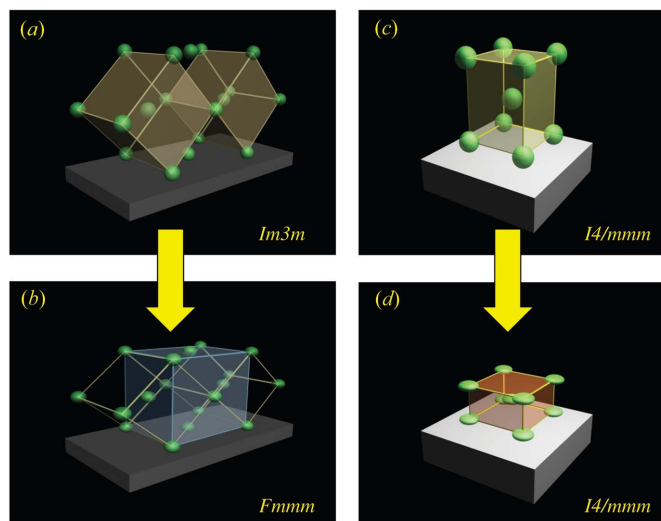


Figure 4 Drawing of the phase transitions observed in dried (333 K) TEOS (a) and MTES-TEOS (c) films and upon calcination at 873 K (b) and (d), respectively.

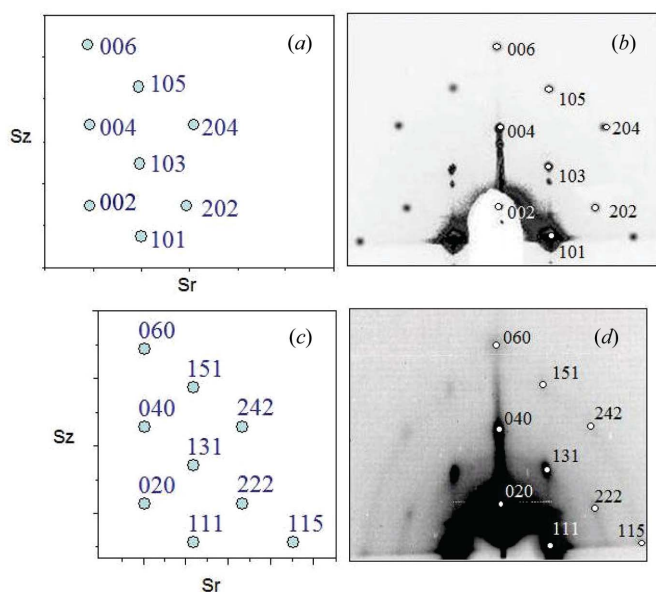


Figure 5 Correspondence between the simulated structure (calculated using the programme *CMPR*) and the measured GISAXS images in MTES-TEOS (a) and (b), and TEOS films (c) and (d), calcined at 473 K.

(which contains a non-hydrolyzable CH_3 group covalently bonded to the Si atom) yields a different mesophase and different phase transitions.

The attribution of these phases has been obtained taking into account the allowed phase transitions from group theory and simulating, through an iterative process, the structure using the programme *CMPR* (<http://www.ncnr.nist.gov/programs/crystallography/software/cmpr>). Fig. 5 shows an example of the correspondence between the simulated and the measured GISAXS images in MTES-TEOS (Figs. 5a and 5b) and TEOS films (Figs. 5c and 5d) calcined at 473 K. The use of different precursors in the starting solution (with different

kinetics of policondensation) involves the formation of two phases with different space groups. Moreover, Fig. 5 clearly shows how the presence of MTES-TEOS influences not only the mesostructure but also the dimension of the ordered domains: the spots in Fig. 5(b) have a less diffuse and more regular shape. The comparison of SAXS and GISAXS images with the simulated structures has also shown to be a reliable procedure for phase identification for mesostructured materials. Its application, as confirmed by TEM analysis, has allowed an unambiguous description of the mesophase observed in self-assembled films.

4. Conclusions

In this article we have presented an application of transmission and grazing-incidence small-angle X-ray scattering to characterize the phase transformation in self-assembled films. These transitions have been unambiguously identified combining SAXS analysis with computer simulation and transmission electron microscopy; these analytical tools are usually employed to study crystalline structures instead of amorphous materials with ordered spatial distribution of pores such as mesostructured porous films.

FIRB Italian projects are acknowledged for financial support (FIRB contract no. RBNE01P4JF). Professor Roberto Paroni (University of Sassari) is gratefully acknowledged for helpful discussions. Michele Rossi and Ing. Michele Ingrassi are acknowledged for the support given to fabricate the dip-coating system.

References

- Amenitsch, H., Rappolt, M., Kriechbaum, M., Mio, H., Laggner, P. & Bernstorff, S. (1998). *J. Synchrotron Rad.* **5**, 506–508.
- Besson, S., Ricolleau, C., Gacoin, T., Jacquiod, C. & Boilot, J.-P. (2003). *Microp. Mesop. Mater.* **60**, 43–49.
- Cagnol, F., Grosso, D., Soler-Illia, G. J. A. A., Crepaldi, E. L., Babonneau, F., Amenitsch, H. & Sanchez, C. (2003). *J. Mater. Chem.* **13**, 61–66.
- Doshi, D. A., Gibaud, A., Goletto, V., Lu, M., Gerung, H., Ocko, B., Han, S. M. & Brinker, C. J. (2003). *J. Am. Chem. Soc.* **125**, 11646–11655.
- Falcaro, P., Costacurta, S., Mattei, G., Amenitsch, H., Marcelli, A., Cestelli Guidi, M., Piccinini, M., Nucara, A., Malfatti, L., Kidchob, T. & Innocenzi, P. (2005). *J. Am. Chem. Soc.* **127**, 3838–3846.
- Falcaro, P., Grosso, D., Amenitsch, H. & Innocenzi, P. (2004). *J. Phys. Chem. B*, **108**, 10942–10948.
- Grosso, D., Babonneau, F., Sanchez, C., Soler-Illia, G. J. A. A., Crepaldi, E. L., Albouy, P. A., Amenitsch, H., Balkenende, A. R. & Brunet-Bruneau, A. (2003). *J. Sol-Gel Sci. Technol.* **26**, 561–565.
- Grosso, D., Babonneau, F., Soler-Illia, G. J. A. A., Albouy, P. A. & Amenitsch, H. (2002). *Chem. Commun.* pp. 748–749.
- Klotz, M., Albouy, P. A., Ayral, A., Ménager, C., Grosso, D., Van der Lee, A., Cabuil, V., Babonneau, F. & Guizard, C. (2000). *Chem. Mater.* **12**, 1721–1728.
- Kundu, D., Zhou, H. S. & Honma, I. (1998). *J. Mater. Sci. Lett.* **17**, 2089–2092.

- Lu, Y., Gangli, R., Drewien, C. A., Anderson, M. T., Brinker, C. J., Gong, W., Guo, Y., Soyez, H., Dunn, B., Huang, M. H. & Zink, J. I. (1997). *Nature (London)*, **389**, 364–368.
- McConnell, G. A. & Gast, A. P. (1996). *Phys. Rev. E*, **54**, 5447–5455.
- Soler-Illia, G. J. A. A., Crepaldi, E. L., Grosso, D., Durand, D. & Sanchez, C. (2002). *Chem. Commun.* pp. 2298–2299.
- Su, Y.-L., Wang, J. & Liu, H.-Z. (2002). *Macromolecules*, **35**, 6426–6431.
- Yao, N., Ku, A. Y., Nakagawa, N., Lee, T., Saville, D. & Aksay, I. A. (2000). *Chem. Mater.* **12**, 1536–1548.
- Yu, K., Wu, X., Brinker, C. J. & Ripmeester, J. (2003). *Langmuir*, **19**, 7282–728.